

THE ORIGIN OF THE TSUNAMI EXCITED BY THE 1989 LOMA PRIETA EARTHQUAKE  
—FAULTING OR SLUMPING—

Kuo-Fong Ma, Kenji Satake and Hiroo Kanamori

Seismological Laboratory, California Institute of Technology

**Abstract.** We investigated the tsunami recorded at Monterey, California, during the 1989 Loma Prieta earthquake ( $M_w=6.9$ ). The first arrival of the tsunami was about 10 min after the origin time of the earthquake. Using an elastic half space, we computed vertical ground displacements for many different fault models for the Loma Prieta earthquake, and used them as the initial condition for computation of tsunamis in Monterey Bay. The synthetic tsunami computed for the uniform dislocation model determined from seismic data can explain the arrival time, polarity, and amplitude of the beginning of the tsunami. However, the period of the synthetic tsunami is too long compared with the observed. We tested other fault models with more localized slip distribution. None of the models could explain the observed period. The residual waveform, the observed minus the synthetic waveform, begins as a downward motion at about 18 min after the origin time of the earthquake, and could be interpreted as due to a secondary source near Moss Landing. If the large scale slumping near Moss Landing suggested by an eyewitness observation occurred about 9 min after the origin time of the earthquake, it could explain the residual waveform. To account for the amplitude of the observed tsunami, the volume of sediments involved in the slumping is approximately  $0.013 \text{ km}^3$ . Thus the most likely cause of the tsunami observed at Monterey is the combination of the vertical uplift of the sea floor due to the main faulting and a large scale slumping near Moss Landing.

Introduction

The Loma Prieta earthquake ( $M_w=6.9$ ) which occurred in the Santa Cruz Mountains, in central California, on October 18, 1989, (Figure 1a) excited tsunamis in nearby Monterey Bay. Nearfield tsunamis are relatively rare in the United States. The 1906 San Francisco earthquake (Lawson et al., 1910), the 1927 Lompoc earthquake, the 1964 Alaskan earthquake, and the 1975 Kalapana earthquake are among the few examples. Since large earthquakes near the coast, either onshore or offshore, can cause serious tsunami hazards, we investigated the tsunami excited by the Loma Prieta earthquake in an attempt to understand the generation mechanism of such nearfield tsunamis.

We will show that two elements contributed to tsunami excitation—the vertical deformation of the sea floor caused by faulting and the secondary submarine slumping presumably caused by shaking.

Data

Figure 1b shows the tsunami recorded on the tide gauge in Monterey Bay. Schwing et al. (1990) describe this instrument as a bubble gauge. We digitized and detrended the record. Figure 1c shows the detrended record for one hour starting from the origin time of the earthquake. The first arrival of the tsunami is about 10 minutes after the origin time of the earthquake, and the peak-to-peak amplitude is about 40 cm.

Copyright 1991 by the American Geophysical Union.

Paper number 91GL00818  
0094-8534/91/91GL-00818\$03.00

Method

Tsunami waveforms are computed either analytically for the case of uniform depth (e.g. Takahashi, 1942; Kajiura, 1963; Ward, 1982; Comer, 1984; Okal, 1988), or numerically for actual bathymetry (Hwang et al, 1972; Houston, 1978; Aida, 1978; Satake, 1985). Since the bathymetry in Monterey Bay is very complex, with a canyon running northeast to southwest (Figure 1a), the assumption of uniform depth is not valid. We used a finite difference method to compute tsunamis in the bay using the actual bathymetry which is known very accurately.

As the initial condition for tsunami computation, we used the vertical ground displacement caused by faulting. For this computation, we used Okada's (1985) program which computes ground deformations caused by faulting in a homogeneous half space. Since the source process time of the earthquake is less than 10 seconds and the water depth is much smaller than the scale length of the ground deformation, we assumed that the water surface is uplifted instantaneously exactly in the same way as the bottom deformation. The amplitude of the tsunami is of the order of 10 cm and is much smaller than the water depth, about 100 m. Also the wavelength of the tsunami, about 10 km in the bay, is much longer than the water depth. Hence we can use the vertically integrated linear long-wave equation and continuity equation as basic equations of tsunami propagation. In a Cartesian coordinate system (x, y) these equations are given by

$$\frac{\partial Q_x}{\partial t} = -gD \frac{\partial H}{\partial x}$$

$$\frac{\partial Q_y}{\partial t} = -gD \frac{\partial H}{\partial y}$$

and

$$\frac{\partial H}{\partial t} = -\frac{\partial Q_x}{\partial x} - \frac{\partial Q_y}{\partial y}$$

where  $Q_x$  and  $Q_y$  are the flow rate obtained by integrating the velocity vertically from the bottom to the surface in the x and y directions respectively, g is the acceleration of gravity, D is the water depth, and H is the water height above the average surface. These equations are solved with a finite difference method. The bathymetry in Monterey Bay and the area for which the computation is made are shown in Figure 1a. The grid size is 1/4 min, which is about 400 m and 500 m in the x and y directions, respectively, and the number of grid points is about 14,400. The time step of computation is 2 sec which is chosen to satisfy the stability condition for the finite difference calculation. Since the bathymetry is known in detail, the tsunami can be computed very accurately.

Fault Model

The fault model of the Loma Prieta earthquake has been determined very well using seismic, geodetic, and aftershock data. Kanamori and Satake (1990) inverted teleseismic body- and surface-wave data and obtained a mechanism with dip= $70^\circ$  SW, rake= $138^\circ$ , and strike= $N128^\circ$  E. The seismic moment is  $3 \times 10^{26}$  dyne-cm ( $M_w=6.9$ ). The total length of the aftershock area is about 40 km, and the main shock is located near the center of the aftershock (U.S.G.S. staff,

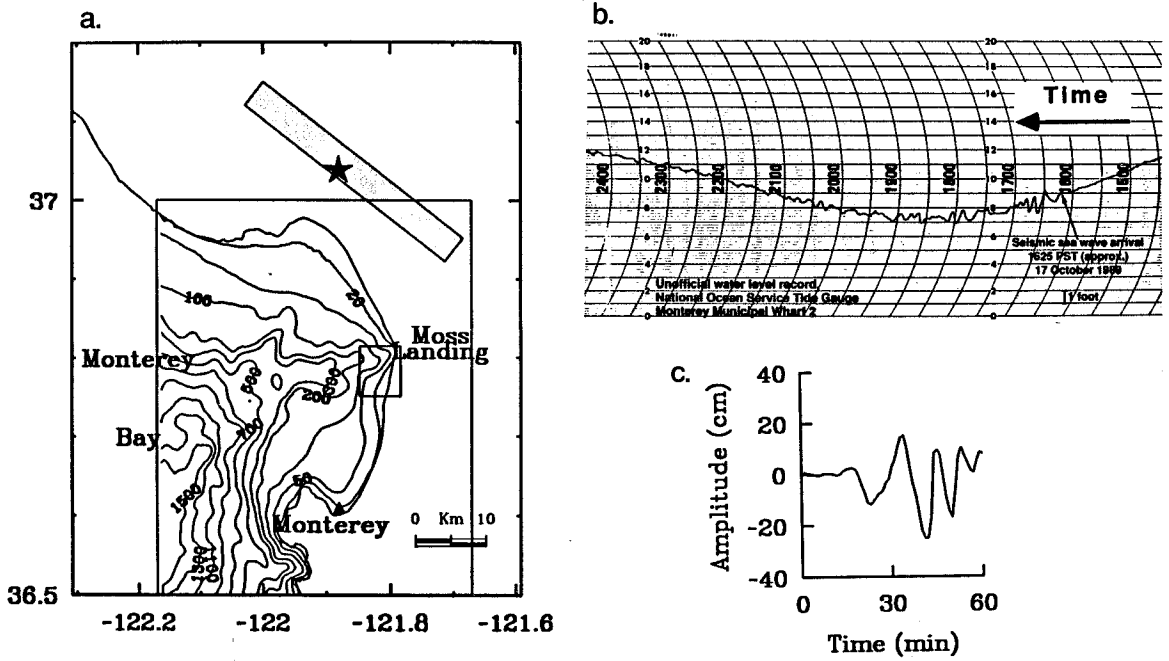


Fig.1 a): Locations of the fault (shaded strip) and the tide gauge station (solid triangle). The star indicates the epicenter of the main shock of the 1989 Loma Prieta earthquake. The bathymetry in Monterey Bay and the area over which the tsunami computation is made are shown in the boxed area. The contour lines indicate the water depths in meters. The shaded box near Moss Landing indicates the location of the subsidence source. b): Tsunami recorded on the tide gauge at Monterey (after Schwing et al., 1990). c): Detrended tsunami record for one hour starting from the origin time of the earthquake.

1990), which suggests bilateral faulting. Kanamori and Satake (1990) suggested a uniform fault model having a fault length,  $L$ , of 35 km. The coseismic slip on the fault is 238 cm, if the fault width,  $W$ , is assumed to be 12 km. Lisowski et al. (1990) compared the observed geodetic data with several dislocation fault models; their preferred fault model has a fault length of 37 km and fault width of 13.3 km. The coseismic slip on the fault is 204 cm. The focal mechanism has dip= $70^\circ$  SW, rake= $144^\circ$ , and strike= $N44^\circ$  W. The total seismic

moment determined from geodetic data is the same as that determined from seismic data by Kanamori and Satake (1990).

Results

We first computed the vertical crustal deformation for the uniform seismic fault model ( $L=35$  km,  $W=12$  km, and  $D=238$  cm) determined by Kanamori and Satake (1990), and used it as the initial condition for tsunami computation. Figure

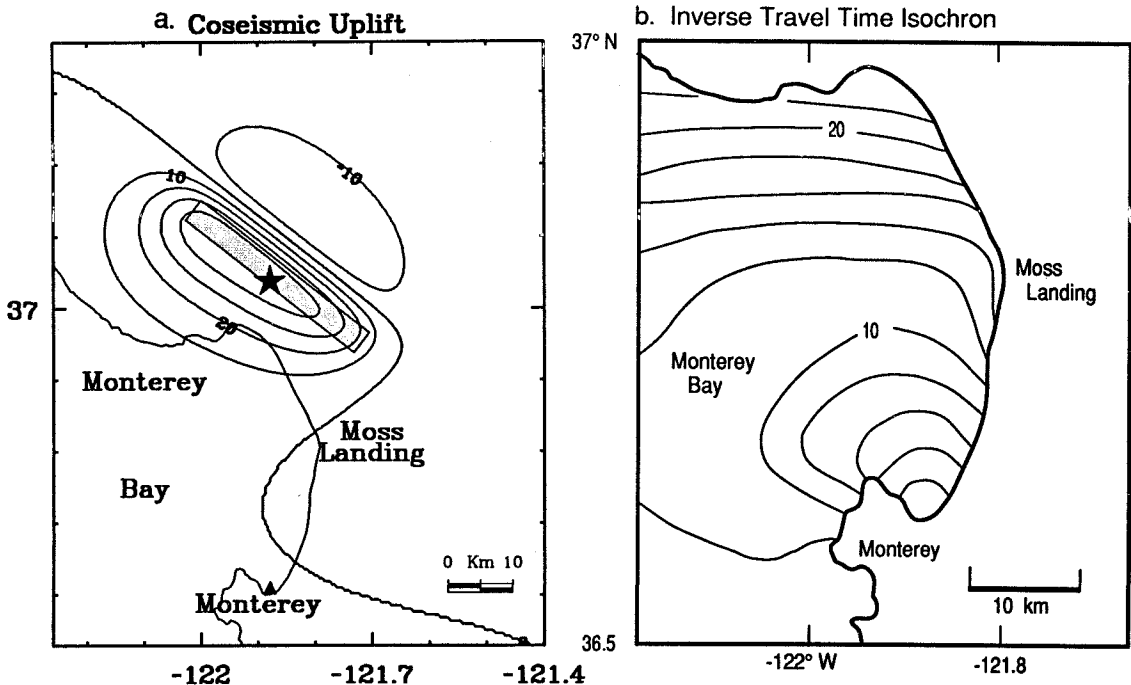


Fig. 2 a): Vertical crustal deformation with 10 cm contour interval for uniform seismic fault model ( $L=35$  km,  $W=12$  km, and  $D=238$  cm). b): Inverse tsunami travel time isochrons. The contour lines indicate the tsunami wavefronts at every 2 min.

2a shows the location of the fault and the vertical crustal deformation. The displacement beneath the sea floor, a maximum of 25 cm, is responsible for tsunami generation.

To see the contribution of the sea-floor displacement to the observed tsunami, we computed an inverse travel-time diagram by the finite difference method by placing a source at the tide-gauge station, and propagating tsunamis backward into the bay. Figure 2b shows the inverse tsunami travel times every 2 min. The isochron at 10 min is close to the southern edge of the displacement field defined by the 0 cm contour line. This is consistent with the onset time of the tsunami at 10 min after the origin time of the earthquake. Figure 3 shows the snapshots of computed tsunamis from the uniform seismic fault model at 5, 10, 15, 20, 25, and 30 min after the origin time.

Figure 4a compares the synthetic tsunami computed for this model with the observed. The synthetic tsunami can explain the arrival time, polarity, and amplitude of the beginning of the observed tsunami. However, the period of the synthetic tsunami is too long compared with the observed.

The reason for the long period of the synthetic tsunami is that the sea floor deformation caused by faulting is very broad, hence the wavelength of tsunami also becomes long as seen in Figure 3. If the slip on the fault is more localized than that in the model used in the above computation, the period of the synthetic tsunami could be decreased. To test this, we computed tsunamis for three localized sources and for the geodetic fault model obtained by Lisowski et al. (1990) for comparison.

In the first case we localized the entire slip in the northwestern half of the fault (fault length=17.5 km). In the second case, the slip is localized in the southeastern half (fault length=17.5 km). In the third case, we localized the displacement in the bottom half of the fault plane (fault length=35 km, width=6 km). In all of these cases, the seismic moment is the same as for the uniform model. These cases represent the three extreme cases of localized sources. The fourth model is taken from Lisowski et al. (1990). Figures 4b to 4e compare the synthetics for these cases with the observed. The waveform of the synthetics is not very different from that for the uniform model. This result indicates that the displacement field caused by faulting is smoothed out in Monterey Bay, and it is not possible to explain the short period of the observed tsunami.

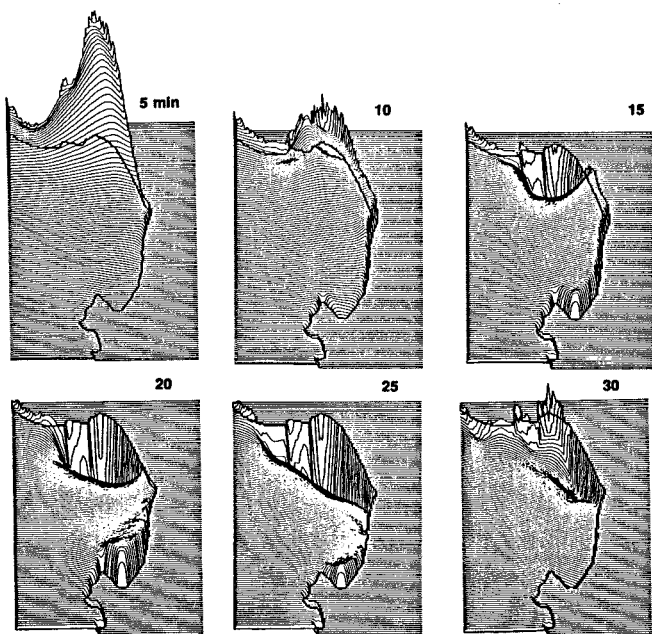


Fig. 3 Snapshots of the computed tsunami computed for the fault model at 5, 10, 15, 20, 25, and 30 min.

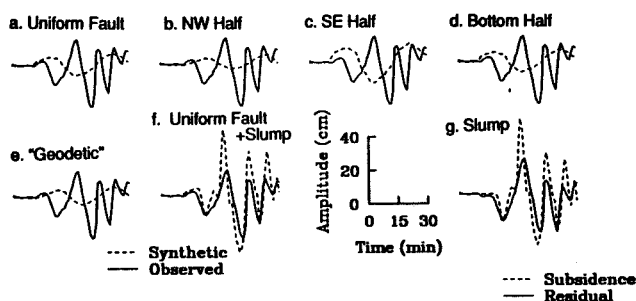


Fig. 4 a), b), c), d), e): Comparison of the synthetic tsunami (dashed line) computed for various fault models with the observed (solid line). f): Comparison of the synthetic tsunami (dashed line) computed for faulting and slumping combined with the observed (solid line). g): Comparison of the residual waveform (observed minus synthetic waveform for uniform seismic fault model, solid line) with the synthetic tsunami computed for a 35 cm subsidence over the shaded area in Figure 1a.

Thus the difference in the period suggests that a secondary source may be responsible for the tsunami observed at Monterey. To explore this possibility, we computed the residual waveform, e.g. the observed minus the synthetic waveforms. The residual waveform, shown in Figure 4g, begins as a downward motion at about 18 min after the origin time of the earthquake. Figure 2b shows that the isochron at 18 min is slightly north of Moss Landing. Schwing et al. (1990) suggest the possibility of large scale slumping near Moss Landing. Sea level fell by 1 m or more near Moss Landing soon after the earthquake. This sea level change is larger than the change expected from solely the direct effect of faulting. The inverse travel time curve shown in Figure 2b suggests that if this slumping occurred 9 min after the earthquake, the arrival time of the residual tsunami shown in Figure 4b could be interpreted as due to the slumping at Moss Landing. In fact a single subsidence source placed in the 39 km<sup>2</sup> square area shown in Figure 1a can produce a tsunami very similar to the residual tsunami, as shown in Figure 4g. The dimension of the subsidence area is adjusted so that the period of the synthetic tsunami agrees with the observed. To match the amplitude of the observed tsunami, a subsidence of 35 cm over the square area is required. Figure 4f compares the synthetic waveform computed for faulting and slumping combined with the observed.

A slump may be most adequately modelled by a sudden subsidence followed by a gradual uplift. However, the details are unknown. If the later uplift was gradual, the tsunami source could be modelled using a single subsidence source. If this is the case, our result suggests that the volume of sediments involved in the slumping is approximately 0.013 km<sup>3</sup>. However, this estimate depends on the details of the slumping. Unfortunately, from the single observation we cannot determine further details.

### Conclusion

The uniform fault model determined from seismic data can explain the arrival time, polarity, and amplitude of the beginning of the observed tsunami, but the period of the synthetic tsunami is too long. We tested fault models with a wide range of nonuniform slip distribution, but none of them could explain the observed period satisfactorily. This suggests that a secondary source is required to explain the tsunami observed at Monterey. The residual waveform, the observed minus synthetic waveform computed for the seismic source, suggests that the most likely secondary source is a sediment slumping near Moss Landing; evidence for such a slumping has been reported by an eyewitness.

Since the tsunami excited by the secondary source can be more extensive than that by the earthquake faulting itself, as is the case for the Loma Prieta earthquake, the possibility of tsunamis caused by secondary sources needs to be carefully evaluated in assessing the tsunami potential of nearshore earthquakes.

**Acknowledgments** This work was supported by the National Science Foundation grant EAR 89-15987 and U.S. Geological Survey grant 14-08-0001-G1832. Contribution No. 4949, Division of Geological and Planetary Sciences, California Institute of Technology, Pasadena, California.

#### References

- Aida, I., Reliability of a tsunami source model derived from fault parameters, J. Phys. Earth, **26**, 57-73, 1978.
- Comer, R. P., The tsunami mode of a flat earth and its excitation by earthquake sources, Geophys. J. R. astr. Soc. **77**, 1-27, 1984.
- Houston, J. R., Interaction of tsunamis with the Hawaiian Islands calculated by a finite-element numerical model, J. Phys. Ocean., 93-102, 1978.
- Hwang, L.-S., H. L. Butler, and D. J. Divoky, Tsunami model: Generation and open-sea characteristics, Bull. Seismol. Soc. Am., **62**, 1579-1596, 1972.
- Kajiura, K., The leading wave of a tsunami, Bull. Earthq. Res. Inst. Univ. Tokyo, **41**, 535-571, 1963.
- Kanamori, H. and K. Satake, Broadband study of the 1989 Loma Prieta earthquake, Geophys. Res. Lett., **17**, 1179-1182, 1990.
- Lawson, A. C., G. K. Gilbert, H. F. Reid, J. C. Branner, A. O. Leuschner, G. Davidson, C. Burkhalter, and W. W. Campbell, The California earthquake of April 18, 1906, report of the state earthquake investigation commission, Carnegie Institution, **2**, 369-373, 1910.
- Lisowski, M., W. H. Prescott, J. C. Savage and M. J. Johnston, Geodetic estimate of coseismic slip during the 1989 Loma Prieta, California, earthquake, Geophys. Res. Lett., **17**, 1437-1440, 1990.
- Okada, Y., Surface deformation due to shear and tensile faults in a half-space, Bull. Seismol. Soc. Am., **75**, 1135-1154, 1985.
- Okal, E. A., Seismic parameters controlling far-field tsunami amplitudes: A review, Natural Hazards, **1**, 67-96, 1988.
- Satake, K., The mechanism of the 1983 Japan Sea earthquake as inferred from long-period surface waves and tsunamis, Phys. Earth Planet. Inter., **37**, 249-260, 1985.
- Schwing, F.B., J. G. Norton and C. H. Pilskaln. Earthquake and Bay, response of Monterey Bay to the Loma Prieta earthquake, EOS, **71**, 250-251, 1990.
- Takahashi, R., On seismic sea waves caused by deformations of the sea bottom, Bull. Earthq. Res. Inst. Univ. Tokyo, **20**, 377-400, 1942.
- Ward, S.N. Earthquake mechanisms and tsunami generation: The Kuril Islands earthquake of 13 October, 1963, Bull. Seismol. Soc. Am., **72**, 759-777, 1982.

H. Kanamori and K.-F. Ma, Seismological Laboratory, 252-21, California Institute of Technology, Pasadena, CA 91125.

K. Satake, Dept. of Geological Sciences, University of Michigan. 1006 C. C. Little Bldg. Ann Arbor, MI 48109-1063

(Received November 19, 1990;  
accepted January 15, 1991.)